AN ELASTIC-PLASTIC CRACK GROWTH ANALYSIS USING THE J-INTEGRAL CONCEPT

J. K. Musuva and J. C. Radon

Department of Mechanical Engineering, Imperial College of Science and Technology, London SW7 2BX, UK

ABSTRACT

An analysis of fatigue crack growth and stable crack growth using the J-integral has been carried out. At low and medium stress intensities the crack growth process appeared to be strain-controlled crack-tip blunting mechanism. However, at high stress intensities the growth was caused by void coalescence and the stable crack growth was derived from J_R-curves. Assuming that these two crack growth mechanisms may act simultaneously and are additive, under elastic-plastic conditions, the total fatigue crack growth was predicted.

KEYWORDS

Elastic-plastic crack growth, J-integral, crack tip blunting, ductile tearing.

INTRODUCTION

Linear elastic fracture mechanics (LEFM) is based on analytical results showing that the crack tip elastic stress field is uniquely characterised by the stress intensity factor, K. This parameter may be used to describe the resistance of metals to both static fracture and fatigue crack growth provided that the crack tip deformations are small. However, substantial limitations on the use of LEFM arise when materials capable of large plastic deformations, such as tough structural steels, are considered. If the plastic deformation around the crack tip is large, the plastic effects are also large and the stress intensity factor, K, loses its original significance. Therefore, under conditions of large plasticity at the crack tip an alternative characterising parameter to K has to be employed.

The J-integral (1) concept has been found to be a satisfactory failure criterion for those materials which fail only after substantial plastic deformation followed by slow stable crack growth. The concept has sometimes been interpreted as a measure of the intensity of the characteristic crack tip strain field (2). This interpretation, similar in philosophy to the LEFM stress intensity parameter, may account for the success of the J-integral as a static and fatigue fracture criterion under elastic-plastic conditions (3-6).

The J-integral was developed for non-linear elastic materials, and for such materials, it can be expressed in terms of the potential energy available for crack extension and discussed later. For the special case of linear elastic materials, J reduces to the strain energy release rate, G. For the elastic case J (or G) is simply related to K and E as follows:

$$J = G = \frac{K^2}{E} \quad \text{for plane stress} \tag{1}$$

$$\text{and} \quad J = G = \frac{(1-\nu^2)K^2}{E} \quad \text{for plain stress} \tag{2}$$

For plastic deformation, J loses its potential energy interpretation, but retains its physical significance as a measure of the crack tip strain field. Therefore, it is not surprising that the J-integral has been shown to be a promising correlation factor for fatigue crack growth under plastic conditions (4-6) in a relationship between da/dN and ΔJ of the form

$$da/dN = C\ (\Delta J)^{m_1} \tag{3}$$

where C and m_1 are constants.

In the present analysis, an attempt will be made to evaluate the above relationship eqn (3) analytically by assuming that a strain field (7) exists around the crack-tip, and also that crack growth occurs when the level of the plastic deformation or the level of strains ahead of the crack-tip will reach the fracture strain of the material, ε_f.

THEORETICAL CONSIDERATIONS

(a) Stress and Strain Fields

Using an earlier analysis by Rice and Rosengren (8) and Hutchinson (9), McClintock (7), derived the stress and strain distribution in terms of J-integral, Fig.2. Applying a method suggested by Lamba (10), the strain distribution at the crack tip, under cyclic loading, can be expressed as:

$$\Delta\varepsilon(x) = 2\,\varepsilon_{yc}\ \left\{\frac{\Delta J}{4\ I_{on}\varepsilon_{yc}\sigma_{yc}x}\right\}^{\frac{1}{n+1}} \tag{4}$$

where I_{on} is a function of the strain hardening exponent, n and of the state of stress at the crack-tip in the direction of crack growth (i.e. $\theta = 0$). The above expression implies infinite strains at the crack-tip which is not the case for ductile engineering materials. To avoid this, a finite opening $2r_c$ (Fig.1) is introduced into the above expression and this can then be rewritten in the form

$$\Delta\varepsilon(x) = 2\,\varepsilon_{yc}\left\{\frac{\Delta J}{4\ I_{on}\varepsilon_{yc}\sigma_{yc}(x + r_c)}\right\}^{\frac{1}{n+1}} \tag{5}$$

(b) Fatigue Crack Growth

The process of crack growth is assumed to occur when the plastic strains at the crack-tip become large, i.e. of the order of the true fracture strain, ε_f. The tip of the originally sharp crack becomes blunted and its flanks, initially closed, will separate by a finite distance yet remaining almost parallel. Further damage occurs only when this separation reaches a critical value, $2r_c$, Fig. 1. Therefore, it will be necessary to define an effective ΔJ, ΔJ_{eff}, at which the crack tip is opened and the material can deform. It is assumed here that deformation does not take place when the crack is closed, nor that the tip resharpens. Also $2r_c$ can be viewed as a critical crack opening displacement below which no sufficient plastic damage occurs at the crack tip to cause further growth. This could be associated with threshold conditions for a non-propagating crack.

Assuming that fatigue crack growth is a cycle by cycle process occuring at the crack tip whenever the above conditions are satisfied, the crack advance per cycle, Δa ($\equiv da/dN$), is given by substituting Δa for x and ε_f for $\Delta\varepsilon(x)$ in eqn (5):

$$\varepsilon_f = 2\,\varepsilon_{yc} \left\{ \frac{\Delta J_{eff}}{4\, I_{on}\, \varepsilon_{yc}\, \sigma_{yc}\, (\Delta a + r_c)} \right\}^{\frac{1}{n+1}} \tag{6}$$

Rearranging, we obtain

$$da/dN = \left(\frac{1}{\varepsilon_f}\right)^{n+1} \frac{(2\,\varepsilon_{yc})^n}{2\,\sigma_{yc} I_{on}}\, \Delta J_{eff} - r_c \tag{7}$$

The value r_c can be arrived at by allowing for $da/dN \to 0$ at a critical value of ΔJ_{eff} designated here $\Delta J_{c,th}$ which is the critical threshold value for a non-propagating crack.

Thus, from eqn (7) we obtain:

$$r_c = \left(\frac{1}{\varepsilon_\ell}\right)^{n+1} \frac{(2\,\varepsilon_{yc})^n}{2\,\sigma_{yc} I_{on}}\, \Delta J_{c,th} \tag{8}$$

and the crack growth rate is given by:

$$da/dN = \frac{2^{n+1}}{4E^n} \frac{\Delta J_{eff} - \Delta J_{c,th}}{I_{on} (\varepsilon_f)^{n+1} (\sigma_{yc})^{1-n}} \tag{9}$$

(c) Crack Growth Evaluation:

At this point, it is necessary to consider the limitations of expression (9) as related to the amount of plastic deformation at the crack tip. The above analysis applies to crack growth by the crack tip blunting mechanism and does not account for any additional crack growth by other mechanisms, such as microvoid

coalescence (11). Therefore, its applications is limited to those regions of LEFM and YFM where the intense zone of deformation, ω, (Fig.2) is small compared with the planar dimensions (12). However, when ω is large the expression (9) would underestimate the actual growth rate.

Athigh stress intensities, the intense zone of deformation has to be taken into account. At present, no simple analysis exists except that by Rice and Johnson (12) who approximated this region using slip-line theory.

There is little doubt that voids will develop in the deformation zone at an early stage.

Subsequent straining will cause increasing crack tip deformation. The lack of analytical solution of this type of intense disturbance may explain why fatigue crack growth models are frequently modified to include an empirical factor in the form of $K_c/(K_c - K_{max})$ in order to account for the growth rates that occur at high stress intensities due to void coalescence, creep and other processes.

At high stress intensities, the crack growth may be estimated using crack growth resistance curves (R-curves) (13). The R-curve may be approximated by (11)

$$\Delta a = C(J_R)^{m_2} \tag{10}$$

where C and m_2 are material constants determined experimentally. It could be reasonably assumed that the crack tip blunting mechanism predominates in crack growth at low stress intensities whereas void coalescence predominates at high stress intensities. Although, there is at present no evidence available to show that these processes are additive, it is suggested that at least at intermediate stress intensities both mechanisms occur simultaneously. Therefore, the total crack growth can be expressed by direct summation of eqns (9) and (10) i.e.

$$(da/dN)_{total} = \frac{2^{n+1}(\Delta J_{eff} - \Delta J_{c,th})}{4(\varepsilon_f)^{n+1}(\sigma_{yc})^{1-n}E^{n}I_{on}} + C(J_{max})^{m_2} \quad . \tag{11}$$

where J_R in eqn (10) is now replaced by J_{max} the maximum value of applied ΔJ.

It may be noted here that the transition region between the true cyclic crack propagation and stable slow growth was investigated by Leevers et al (14) using polymers at room temperature and wide range of frequencies. In that study the high stress intensity cyclic growth was successfully predicted from data obtained under static loads. It could be speculated therefore that a similar approach could be applied in ductile metals.

DETERMINATION OF J FOR COMPACT SPECIMENS

In the last few years, the experimental techniques for the determination of the

J-integral have substantially improved. Begley and Landes (2) attempted an experimental determination of J based on the energy release rate interpretation (1) expressed as:

$$J = -\frac{1}{B}\frac{dU}{da} \tag{12}$$

where B is the specimen thickness, U the potential energy and a the crack length. This technique, is slow and tedious and has now been superseded by simpler procedures (3). For deeply cracked bend and compact specimens, the J-integral can be approximated from the load vs load-point displacement curve as proposed by Rice et al (15), namely,

$$J = \frac{2A}{B\,(W-a)} \tag{13}$$

where W is the specimen width, and A is the area under the load vs load-point displacement curve at a given displacement, Fig.3(a)Further analysis (16,17) has shown that eqn (13) is slightly inaccurate for compact specimens over the a/W range normally used in fracture toughness tests and the improved form is:

$$J = \frac{\lambda A}{B(W-a)} \tag{14}$$

where λ takes into account a correction for the tension component in loading. The values of λ as tabulated in (17), have been used in the present investigation for the estimation J, though a value of $\lambda = 2.18$ as suggested in (16) for $a/_W > 0.6$, was used for earlier analysis (4).

As the deformation theory of plasticity, on which the J-integral concept is based, does not directly account for the plasticity effects observed on unloading, there may be some doubt concerning J-integral applicability to cyclic loading (3). However, recent applications for elastic-plastic fatigue crack growth (4-6) have shown encouraging results. Assuming that the major part of fatigue crack growth takes place during loading, then ΔJ can be estimated from load vs load-point displacement hysteresis loops, Fig 3(b), (5).

EXPERIMENTAL PROCEDURE AND RESULTS

The material investigated was a low alloy steel, BS 4360-50D, of chemical composition and mechanical properties as given in Table 1, available in three thicknesses, 12 mm, 24 mm, and 50 mm.

The experimental procedure and data reduction techniques used have been described elsewhere (4) in a more detailed form. However, it is worth mentioning here that compact specimens were adequately modified to facilitate measurement of deflections using a standard clip gauge. J and Δ J values were determined from the areas under the load-displacement curves with the help of a planimeter. Typical curves derived in the monotonic and cyclic tests are shown in Figs 4 and

5 respectively. The crack increments, Δa, were determined using the unloading compliance method (3) for both types of tests. A calibration curve, Fig. 6, was found to conform to the data recently derived by Saxena and Hudak (18). However, a few additional J-tests were made using the multispecimen method (3).

The results for the stable crack growth under monotonic loading are plotted in Fig. 7. The results show a linear relationship for low crack extensions and these can be fitted by a mean R-curve in the form:

$$\Delta a = 7.5 \times 10^{-18} J_R^{2.60} \qquad (15)$$

At higher growth rates, great scatter and also deviation from linearity sets in and this seems to be most prominent in the thinner specimens.

The results for the cyclic elastic-plastic tests are presented in Fig.8. These results show that growth rates are higher in the thicker material though the difference in growth rates is not very significant as was found at lower growth rates (19,20). It will be noted that at growth rates above 3×10^{-3} mm/cycle, the stable crack growth by ductile tearing strongly interferes with the true cyclic growth. At these growth rates, the cyclic growth data correspond to the crack growth extrapolated from the stable crack growth. This trend seems to confirm that cyclic growth at high stress intensities is essentially by void coalescence.

In order to evaluate eqn (11) for the total crack growth, the following material constants were used for BS 4360-50D: true fracture strain, $\varepsilon_f = \ell n \left(\frac{100}{100 - \psi}\right)$ where ψ (% reduction in area) is 74%. Thus $\varepsilon_f = 1.35$; E and Poisson ratio, ν, were taken as 207×10^9 N/m², and 0.3 respectively and σ_{yc} is 425 MN/m². The value of I_{on} is a function of state of stress at the crack-tip.

For small scale yielding and under plane strain conditions $I_{on} = 22.38$, using the expression $I_{on} = \pi (1+n)/(1-2\nu)^2$ (11, 20), where n is 0.14.

Fig. 9 shows the elastic-plastic crack growth data together with the predicted growth rates by eqns (9), (15) and (11). It will be noted that although a very simplified crack growth model involving superposition of two growth mechanisms has been used, the prediction is good. Fig. 9 indicates that the blunting mechanism is dominant at low stress intensities, whereas at high stress intensities void coalescence involving dimple formation and ductile tearing becomes the principal factor. The data for the whole range of growth rates from threshold to fast fracture are presented in Fig.10. Eq (11) is seen to fit the data fairly well.

Fractographic examination of fracture surfaces revealed both striations, which are a feature of the blunting mechanism, and ductile ruptures with micro-branching, which are a result of void coalescence.

Fig. 11(a) shows a micrograph taken from a region of growth rates of the order of 1.5×10^{-4} mm/cycle c.f. fig. 8. In this region and also at lower growth rates, striations were found to dominate the area of the fracture surface. However

at higher growth rates such as 10^{-3} mm/cycle, Fig.11(b), areas of ductile tearing, may be observed. There is some evidence available to show that these areas increase with increasing growth rates. At still higher growth rates the dimple formation is predominant Fig.11(c). It should be noted that at very low stress intensities, near the threshold, the striations were found to disappear from the fracture surface and were replaced gradually by areas of quasi-cleavage associated with environmental effects.

DISCUSSION

The process of crack growth is assumed to begin when the plastic strains near the crack tip become large, i.e. of the order of the true fracture strain of the material. Before this process begins, the crack has to open and blunt to a critical finite separation; the growth does not occur while the crack is closed.

When the applied stress intensity is large enough, microvoids initiate in the regions of weak secondphase particles or inclusions. These then grow by plastic deformation and coalese by ductile rupture or cleavage, and the crack extends further into the material. This sequence of crack tip extension is schematically illustrated in Fig.1. The crack tip deformation and growth by blunting is similar to that discussed by Kuo and Liu (21) who proposed the unzipping model for crack opening and advance.

It will be realised that the strain-controlled criterion for fracture described above has also some limitations. It assumes a homogeneous, ductile material undergoing large plastic deformations. If the material contains brittle inclusions, particles or embrittled grain boundaries, the fracture process will be accelerated by superimposed cleavage. At high stress intensities, the growth and coalescence of microvoids will also cause crack growth acceleration which can not be predicted by the strain-controlled blunting mechanism. It may be recalled that in the LEFM (eq9)implies a da/dN vs ΔJ relationship with the value of the exponent, m_1 (eqn 3) of the order of 1. This implies that when m_1 equals 1, the crack growth mechanism is predominantly that of blunting. This process has been actually observed in the high toughness steels and aluminium alloys. In these materials the striation spacing distance equals the macroscopic crack growth rate. On the other hand, in the low toughness materials with high values of m_1, fractographic analyses have revealed striation spacing with superimposed cleavage and intergranular separation as well as void coalescence, (22). Such fracture modes cannot be analysed accurately by current plasticity theories (12,13) and the use of R-curves is particularly convenient.

The stress and strain distribution assumed in the analysis can only be evaluated for either plane strain or plane stress. However, in most practical cases, and specially under elastic-plastic conditions, the state of stress is of mixed mode. Consequently, the function I_{on} in eqn (9) varies with J as it is most likely that the stress state will change from plane strain at low stress intensities, to plane stress at high stress intensities.

Despite the limitations discussed in the previous paragraphs, the results appear to be satisfactory. The correlation of data in Fig. 10 is similar to that provided by Dowling (5), both confirming the applicability of J-integral analysis for cyclic loading. The apparent crack growth acceleration at growth rates above 3×10^{-3} mm/cycle in the results reported here is also present in (5) at growth

rates above 10^{-2} mm/cycle. Crack growth at these high growth rates would be expected to be sensitive to strain rate and the mode of loading.

The present results were obtained at low stress ratios of R < 0.1. It was noted that although crack closure effects were significant at low stress intensities (23), where closure occurred at positive applied loads, at high stress intensities discussed here, the crack needed compressive loads to close. The effects of thickness and stress ratio found at low stress intensities were adequately accounted for in (20) and a complete master curve of da/dN vs ΔJ_{eff} is presented in Fig.10.

Looking now briefly at the crack growth results obtained in the monotonic tests, Fig.7, it is seen that at large crack extensions, crack growth apparently decelerated with increasing J. This behaviour has also been reported by Schwalbe (11) and is due to the development of shear lips. The effect is most significant in the thinner sections where shear lips are likely to cause the thinning out of the specimen thickness. The extrapolation of the R-curve to the region of low growth rates would be justified only if this would not go beyond the threshold for dimple formation. This value may be related to the initiation (J_{ic}) of stable crack growth under plane strain conditions, existing at the centre of the specimen (11). For this material, a J_{ic} value of about 50 x 10^3 N/m was estimated (4).

Finally it should be noted that Herman and Rice (24) reported theoretical and experimental results obtained in elastic-plastic plane strain crack growth. Their theory is based on an asymptotic analysis of crack surface opening and strain distribution at a quasi-statically advancing crack tip in an ideally-plastic solid. The possibility of applying this approach to the present work is being explored.

CONCLUSIONS

The fatigue crack growth and stable crack growth under monotonic loading in BS 4360-50D steel have successfully been analysed using the J-integral and assuming a strain-controlled failure criterion. From the analysis it can be concluded that:

(1) the J-integral can be used to characterise crack growth under both monotonic and cyclic loading.

(2) From fractographic examination, crack growth at medium growth rates (10^{-5} - 10^{-4} mm/cycle) is predominantly by the crack tip blunting mechanism. At high growth rates (> 10^{-2} mm/cycle) growth is dominated by void coalescence, and this can be adequately predicted using R-curves.

(3) For low alloy steels, the elastic-plastic cyclic crack growth can be described in the following terms.

$$(da/dN) = \frac{2^{n+1}\,(\Delta J_{eff} - \Delta J_{c,th})}{4\,(\varepsilon_f)^{n+1}(\sigma_{yc})^{1-n} E^n I_{on}} + C(J_{max})^{m_2}$$

where n is the cyclic strain hardening exponent, ε_f is the true fracture strain σ_{yc} is the cyclic yield stress, I_{on} is a function of the form $\pi(1+n)/(1-2\nu)^2$ for small scale yeilding, $\Delta J_{c,th}$ is the threshold value of ΔJ, J_{max} is the maximum applied ΔJ and ΔJ_{eff} is the value of ΔJ corrected for crack closure. The constant C and m^2 are derived experimentally from the J_R curve.

(4) Further evidence of the additive character of the crack tip blunting and void coalescence mechanisms is necessary.

REFERENCES

1. Rice, J.R. "A Path Independent Integral and the Approximate Analysis of Strain Concentration by Notches and Cracks", J. Appl. Mech. Vol.35, pp 379 - 386 (1968).
2. Begley, J.A. and Landes, J.D. "The J-integral as a Fracture Criterion" in Fracture Toughness, ASTM STP 514, American Society for Testing and Materials, pp 1-23 (1972).
3. de Castro, P.M.S.T., Radon, J.C. and Culver, L.E. "J-resistance curve and ductile tearing of a mild steel", Int. J. Fatigue, Vol.1, pp 153-158 (1979).
4. Musuva, J.K. and Radon, J.C. "Size Effects and the J-integral Approach to low cycle Fatigue Crack Growth" DVM Stuttgart, pp 479-494 (1979).
5. Dowling, N.E. and Begley J.A. (1976). "Fatigue Crack Growth during Gross Plasticity and the J-integral". Mechanics of Crack Growth, ASTM STP 590, American Society for Testing and Materials, pp 82-103.
6. Branco, C.M., Radon, J.C. and Culver, L.E. "Elastic-plastic Fatigue Crack Growth under Load Cycling", J. Strain Analysis Vol.12, pp 71-80 (1977).
7. McClintock, F.A. (1971). "Plasticity Aspects of Fracture", in Fracture: An Advanced Treatise Ed. Liewbowitz H., Vol.3, pp 47-225.
8. Rice, J.R. and Rosengren, G.F. (1969). "Plane Strain Deformation near a Crack-Tip in a Power-law Hardening Material", J. Mech., Phys. Solids, Vol.16, No.1, pp 1-12.
9. Hutchinson, J.W. (1968) "Plastic Stress and Strain Fields at a Crack-Tip" J. Mech.Phys. Solids, Vol.6, No.5,pp 337-347.
10. Lamba, H.S. (1975). "The J-integral Applied to Cyclic Loading", Engng. Fracture Mech., Vol.7, pp 693-703.
11. Schwalbe, K.H. (1979). "Some Properties of Stable Crack Growth", Engng. Fract.Mech., Vol.11, pp 331-342.
12. Paris, P.C. (1977). "Fracture Mechanics in the Elastic-Plastic Regime", Flow Growth and Fracture, ASTM STP 631, American Society for Testing and Materials, pp 3-27.
13. Rhodes, D., Radon, J.C. and Culver, L.E. "Cyclic and monotonic crack propagation in a high toughness aluminium alloy". In print, Int.J.of Fatigue, (1980)
14. Leevers, P.S., Culver, L.E. and Radon, J.C. "Fatigue crack growth in PMMA and rigid PVC under biaxial stress" Engng. Fract.Mech. Vol.11, pp 487-498 (1979).
15. Rice, J.R., Paris P.C. and Merkle, J.G. (1973). "Some Further Results of J-Integral Analysis and Estimates" in Progress in Flaw Growth and Fracture Toughness Testing, ASTM STP 536, American Society for Testing and Materials, pp 231-245.
16. Hickerson, J.P. Jr. "Comparison of Compliance and Estimation Procedures for Calculating J-Integral Values " in Flaw Growth and Fracture, ASTM STP 631, American Society for Testing and Materials, pp 62-71, (1977).
17. Clarke, G.A. and Landes, J.D. "Evaluation of the J-Integral for the Compact Specimens", J. of Testing and Evaluation, JTEVA, Vol. 7, No. 5, pp 264 - 269 (1979).
18. Saxena, A. and Hudak, S.J.Jr. "Review and extension of compliance information for common crack growth specimens". Int.J.Fract. Vol.14, No.5, pp 453-468 (1978).

19. Musuva, J.K. and Radon, J.C. "The Effects of Stress Ratio and frequency on Fatigue Crack Growth". Fatigue of Engng. Mater. and Structures, Vol.1, pp 457-470 (1979).
20. Musuva, J.K. and Radon, J.C. "Analysis of Slow Fatigue Crack Growth and Thresholds in Steels". To be presented at the Int.Eng. "Fatigue 81" in Warwick, UK, 1981.
21. Kuo, A.S. and Liu H.W. "An Analysis of Unzipping Model for Fatigue Crack Growth", Scripta Metal., Vol. 10, pp 723-782 (1976).
22. Tien, J.K. and Purushothaman, S. (1978). Generalised Theory of Fatigue Crack Propagation: Part II - Derivation of Threshold and Paris Regime Crack Growth Rates", Mater.Sci. and Engng., Vol.34, pp 247-262.
23. Elber W. "The Significance of Fatigue Crack Closure" ASTM STP 486, pp 230-242 (1971).
24. Hermann, L. and Rice, J.R. "Comparison of Experiment and Theory for elastic-plastic plane strain crack growth" Proc.Conf. on Micromechanics of Crack Extension (Mechanics and Physics of Fracture II), Churchill College, Cambridge U.K., (April 1980).

(a) Chemical Composition (Weight)

Element	C	Si	Mn	P	S	Cr	Mo	Ni	Al	Cu	Nb
%	0.180	0.36	1.40	0.018	0.003	0.11	0.020	0.095	0.035	0.16	0.039

(b) Mechanical Properties

	Direction		
	Longitudinal	Transverse	Through Thickness
Yield strength (MN/m^2)	386	382	388
Ultimate tensile strength (MN/m^2)	560	551	563
% elongation (GL equal 3")	30	29	18
% reduction in area	74	68	61

Table 1 : Steel BS4360-50D

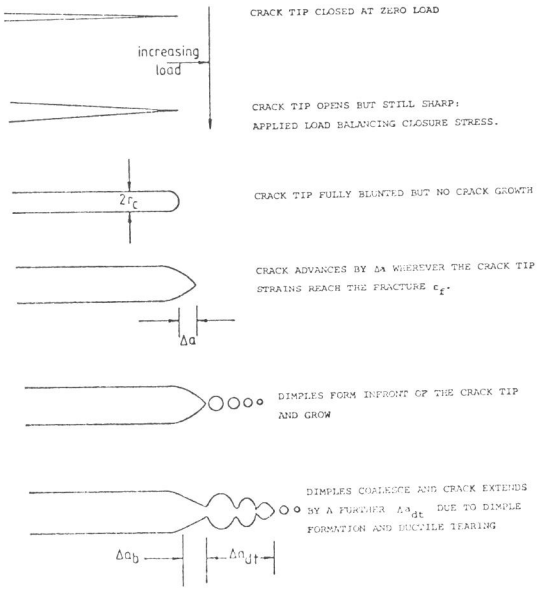

Fig.1 Crack-tip deformations under increasing load.

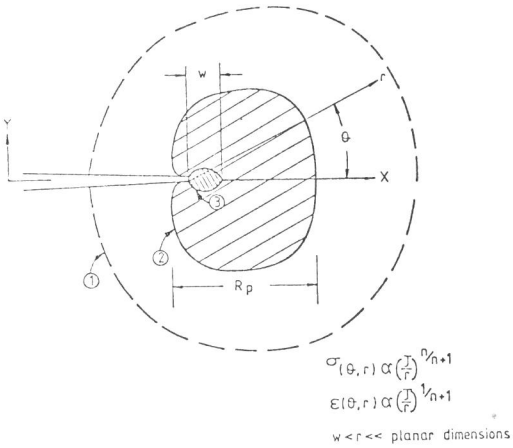

Fig. 2 Crack-tip stress and strain fields.

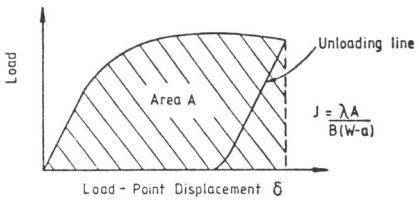

Fig.3(a) Monotonic load vs. displacement curve. Schematic.

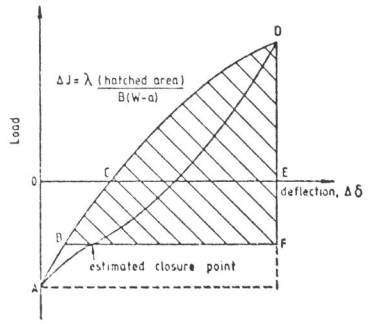

Fig.3(b) Operational definition of 'ΔJ' (Ref.5)

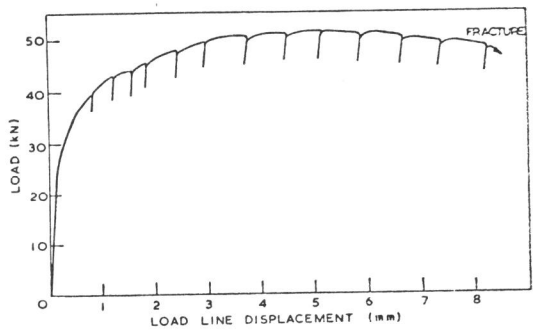

Fig.4 J-test: Single specimen method

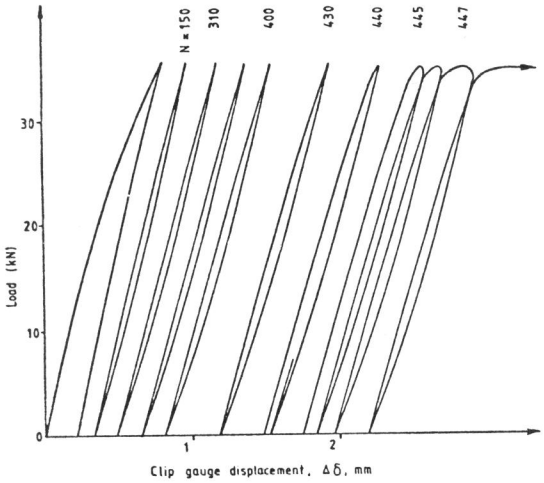

Fig.5 Hysteresis loops in load cycling

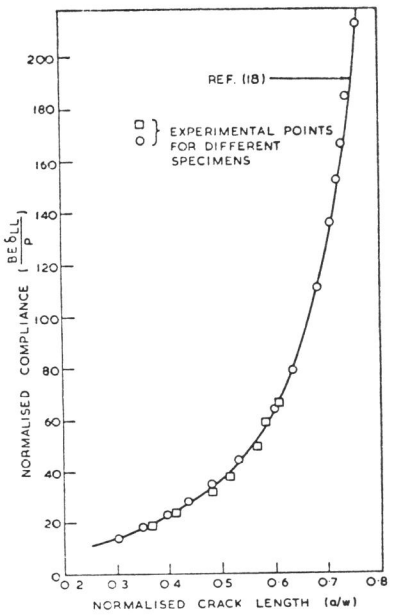

Fig.6 Compliance calibration curve for CTS.

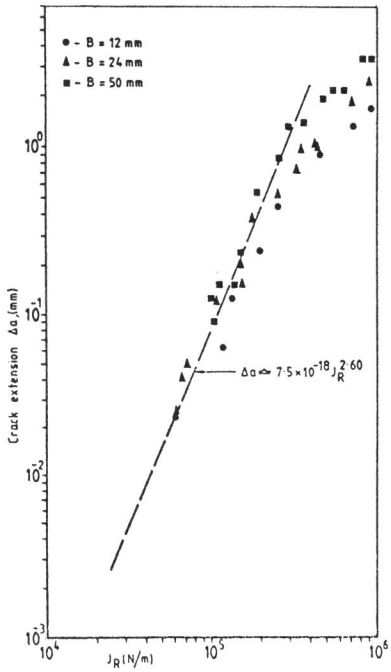

Fig.7 BS4360-50D Monotonic crack growth.

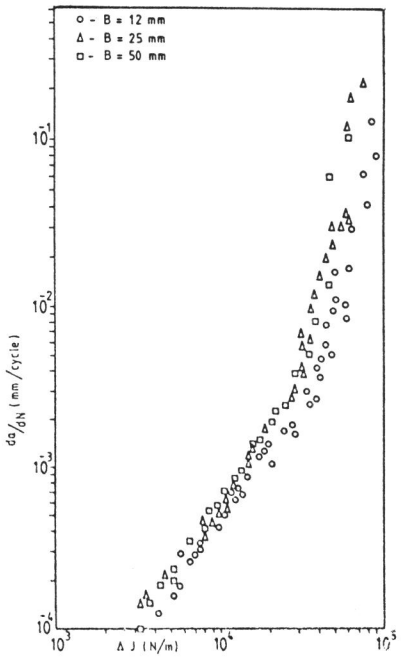

Fig.8 BS4360-50D: Elastic-plastic fatigue crack growth.

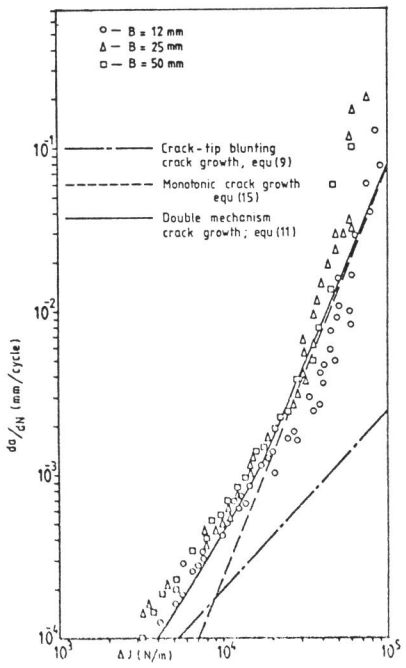

Fig.9 BS4360-50D: Elastic-plastic fatigue crack growth modelling.

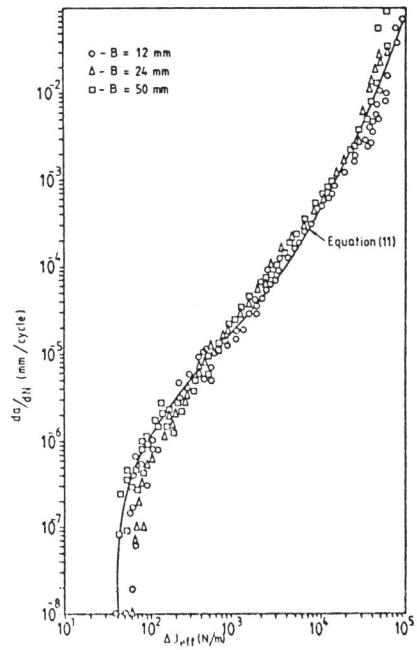

Fig.10 BS4360-50D: da/dN vs. ΔJ_{eff}

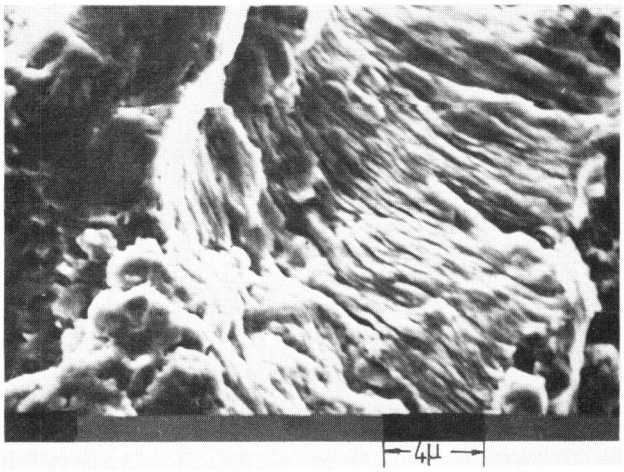

(a) Striations

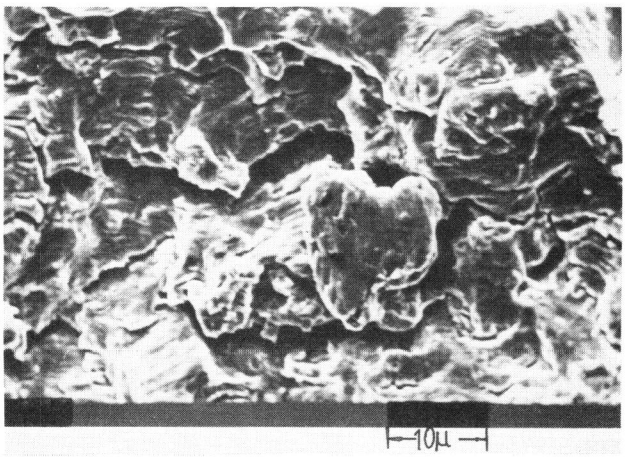

(b) ductile tearing with areas of striation.

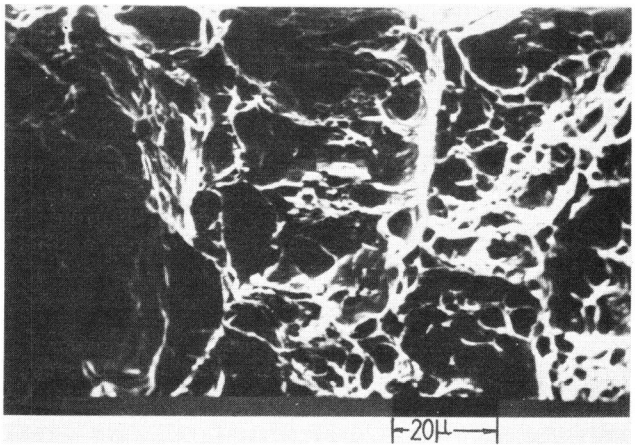

(c) dimples at high stress intensities.

Fig. 11 Micrographs